BMB
Reports

BMB Rep. 2014; 47(2): 92-97
www.bmbreports.org

Sequence-specific interaction between ABD-B homeodomain and *castor* gene in *Drosophila*

*Keon-Hee Kim & Siuk Yoo**
Department of Life Sciences, College of Sciences, Yeungnam University, Gyeongsan 712-749, Korea

We have examined the effect of bithorax complex genes on the expression of *castor* gene. During the embryonic stages 12-15, both *Ultrabithorax* and *abdominal-A* regulated the *castor* gene expression negatively, whereas *Abdominal-B* showed a positive correlation with the *castor* gene expression according to real-time PCR. To investigate whether ABD-B protein directly interacts with the *castor* gene, electrophoretic mobility shift assays were performed using the recombinant ABD-B homeodomain and oligonucleotides, which are located within the region 10 kb upstream of the *castor* gene. The results show that ABD-B protein directly binds to the *castor* gene specifically. ABD-B binds more strongly to oligonucleotides containing two 5'-TTAT-3' canonical core motifs than the probe containing the 5'-TTAC-3' motif. In addition, the sequences flanking the core motif are also involved in the protein-DNA interaction. The results demonstrate the importance of HD for direct binding to target sequences to regulate the expression level of the target genes. [BMB Reports 2014; 47(2): 92-97]

INTRODUCTION

Homeotic/Hox genes were first identified in *Drosophila*, and encode transcription factors that play a pivotal role in giving a unique identity to each segment, thereby setting up morphogenesis along the anterior-posterior axis. The homeotic genes are evolutionarily conserved in organisms ranging from cnidarians to mammals (1). Loss-of-function mutants transform one segment into a copy of another segment (2, 3). In *Drosophila*, homeotic cluster consists of eight genes which are divided into two groups: Antennapedia complex (ANTP-C) and Bithorax complex (BX-C), on the third chromosome. In the BX-C, *Ultrabithorax* (*Ubx*), *abdominal-A* (*abd-A*), and *Abdominal-B* (*Abd-B*) are responsible for determining the identity of thoracic and abdominal segments (4, 5).

The homeotic genes contain a highly conserved 180-bp homeobox encoding homeodomain (HD), a DNA-binding domain consisting of 60 amino acid residues. Although the primary amino acid sequences are different from Hox proteins, the three-dimensional structures are very similar, representing a well-conserved mode of HD-DNA interaction during evolution (1). The HD consists of a flexible N-terminal arm and three α-helices (6). The N-terminal arm is positioned in the minor groove, and is required for the specificity of the protein action. The second and third helices of the HD fold into a conformation similar to the helix-turn-helix DNA-binding motif, and bind in the major groove of the DNA, making them essential for DNA binding (6).

HD proteins recognize a canonical core sequence 5'-TAAT-3', which plays a major role in determining high binding affinity with an approximate K_d value of 10^{-8} to 10^{-11} M, and regulate the expression of a target gene acting either as an activator or a repressor (7-9). In contrast, ABD-B HD binds preferentially to a sequence with an unusual 5'-TTAT-3' core motif instead of 5'-TAAT-3' for other HD proteins (10). It has been reported that the 10 bp sequence (5'-TTTTATGGCC-3') is the optimal DNA binding site for the ABD-B HD, and the N-terminal arm of ABD-B HD is responsible for the sequence-specific binding (11).

ABD-B protein is expressed in the ectoderm and mesoderm of parasegments 13-15, and strongly expressed in the parasegment 14 central nervous system (CNS) at germband retraction (12, 13). Therefore, ABD-B functions primarily to assign identities to parasegments 10 to 14, and it is also involved in the formation of CNS (14).

Castor protein contains a zinc finger domain, and is expressed in a restricted set of neuroblasts and glia in the cephalic regions and the ventral nerve cord (15). A loss-of-function mutation of *castor* results in alterations to gene expression in CNS, followed by defects in axonogenesis (16). The *castor* is also involved in the development of mushroom body in post-embryonic stages (15), and in neuronal differentiation (17). The expression level of the *caster* transcripts is the highest in the CNS of embryos at stage 14, and is detectable only in a few cells of the thoracic and terminal abdomen in stage 15 embryos (16, 18). Recently, the roles of BX-C genes in the regulation of *castor* expression have been studied using anti-

*Corresponding author. Tel: +82-53-810-2378; Fax: +82-53-810-4618; E-mail: yoosiuk@ynu.ac.kr

http://dx.doi.org/10.5483/BMBRep.2014.47.2.117

Received 22 May 2013, Revised 6 June 2013, Accepted 12 June 2013

Keywords: *Abdominal-B*, *Castor*, EMSA, Homeodomain, Homeotic gene

ISSN: 1976-670X (electronic edition)

body staining and *in situ* hybridization. The *Ubx* and *abd-A* genes negatively regulated *castor* expression, whereas the relationship between ABD-B and *castor* was positive (18).

In this study, to determine the effect of *Ubx*, *abd-A*, and *Abd-B* on *castor* expression, the expression levels of *castor* during embryogenesis were examined using real-time PCR. The results showed that the expression of *castor* was positively regulated by *Abd-B*, in contrast to *Ubx* and *abd-A*, which regulate *castor* expression negatively. The relationship between BX-C genes and *castor* are not changed during the embryonic stages 12 through 15. We also demonstrated that the recombinant ABD-B HD specifically binds to the upstream promoter sequence of *castor*, implying that ABD-B directly regulates the expression of the *castor* gene.

RESULTS AND DISCUSSION

Regulation of *castor* gene expression by Bithorax complex

The segment-specific expression patterns of *castor* suggest that its expression is regulated by BX-C. Therefore, in order to investigate the effect of BX-C on the expression of the *castor* gene, we generated BX-C mutant lines and measured the transcript level of *castor*. For the homozygous null mutant embryos for bithorax genes, the *TM1* balancer chromosomes in BX-C mutant lines were replaced by *TTG* balancer chromosomes, and the null embryos lacking a fluorescence signal were collected. For overexpressing BX-C genes, *sca-GAL4* was crossed with each *UAS-Ubx*, *UAS-abdA*, or *UAS-AbdB* line.

Total RNAs were extracted from the embryos either lacking or overexpressing BX-C genes at stage 15, and real-time PCR was carried out using the primers for BX-C genes and *castor* (Supplementary Table 1). The expression levels of BX-C genes

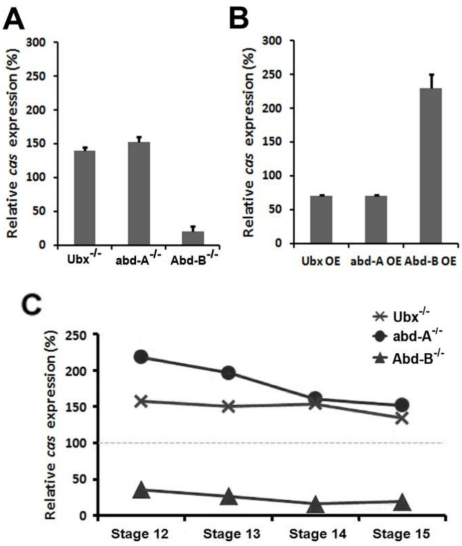

Fig. 1. Expression levels of *castor* (*cas*) transcripts determined by real-time PCR. Total RNAs were extracted from stage 15 embryos in which each BX-C gene is mutated or overexpressed. The expression levels of each gene were compared to that in wild-type embryos. (A) Relative expression levels of castor in *Ubx*$^{-/-}$, *abd-A*$^{-/-}$, and *Abd-B*$^{-/-}$ mutant embryos. In contrast to up-regulation of *castor* in *Ubx*$^{-/-}$ and *abd-A*$^{-/-}$ embryos, the expression of *castor* was down-regulated in *Abd-B*$^{-/-}$ mutant embryos. (B) Relative expression levels of *castor* upon overexpression (OE) of BX-C genes. To overexpress bithorax genes, *sca-GAL4* was crossed with *UAS-Ubx*, *UAS-abdA*, or *UAS-AbdB* line. Expression of *castor* was decreased in both *Ubx* and *abd-A* overexpressing embryos, but it was increased in *Abd-B* overexpressing embryos. (C) Relative expression levels of *castor* in BX-C mutant embryos at stages 12 through 15. Expression of *castor* transcript did not depend on embryonic stage. The means and standard deviations from three independent experiments are shown.

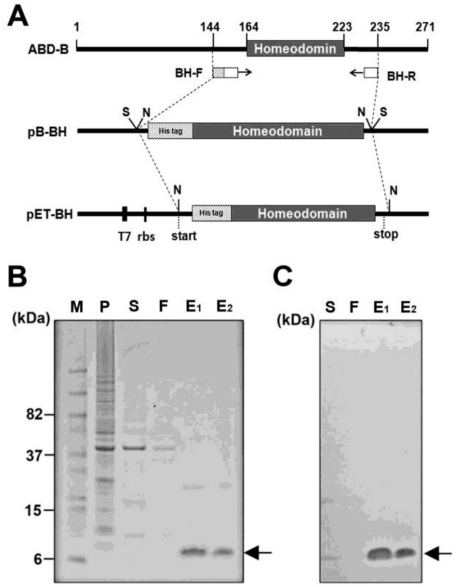

Fig. 2. Purification of the recombinant ABD-B homeodomain. (A) Schematic diagram of plasmid constructs. DNA fragment encoding ABD-B HD and flanking sequences (corresponding to amino acid residues 144-235) was amplified by PCR using BH-F and BH-R primers. The fragment was sub-cloned into *Sma*I site of pBlueScript SK vector to generate pB-BH plasmid. After digestion with *Nde*I, the fragment was cloned into *Nde*I site of pET30b expression vector to generate pET-BH construct. Both primers include *Nde*I site at the 5' end, and BH-F primer contains His·tag. The numbers above the line indicate the position of amino acid residue. Black box, homeodomain; dotted box, histidine tag; white box, primer; N, *Nde*I site; S, *Sma*I site; T7, binding site for T7 RNA polymerase; rbs, ribosome binding site; start, start codon; stop, stop codon. (B) SDS-PAGE showing the recombinant protein purified using nickel-chelating affinity chromatography. *E. coli* carrying pET-BH plasmid was sonicated, and centrifuged to separate pellet (P) from soluble (S) fraction. S fraction was loaded on a column, and the recombinant protein was eluted (E_1 and E_2). M is molecular size marker, and F represents the filtrate through the column. (C) Immunoblot of the same protein samples as in (A). The recombinant ABD-B HD indicated by the arrows in (B) was detected by antibody against histidine tag.

were decreased or increased by more than 3-fold in BX-C mutants or overexpressing embryos, respectively, compared to those in wild-type embryos (data not shown). The *castor* expression was increased in *Ubx* and *abd-A* mutant embryos, whereas it was decreased in *Abd-B* mutant embryos (Fig. 1A). Conversely, the ectopic expression of *Ubx* and *abd-A* suppressed the expression of the *castor* gene, but *Abd-B* enhanced the *castor* transcript level by approximately 2.5-fold (Fig. 1B). These results clearly demonstrate the positive regulation of ABD-B and the negative regulation of UBX and ABD-A on *caster* gene expression.

Since the expression patterns of *castor* are dramatically changed during stages 14 and 15 (18), we further examined whether the effect of BX-C on *castor* gene expression is dependent on the developmental stage. The BX-C mutant embryos were collected at each developmental stage from 12 to 15, and the *castor* transcript level was measured. The result displayed that the *castor* expression was up-regulated in both $Ubx^{-/-}$ and $abd\text{-}A^{-/-}$ embryos, and down-regulated in $Abd\text{-}B^{-/-}$ embryos during stages 12 through 15, implying that the action of BX-C on *castor* expression is not stage-specific (Fig. 1C).

Taken together, in agreement with a previous study (18), these results suggest that both UBX and ABD-A act as repressors, whereas ABD-B acts as an activator to control *castor* expression.

Preparation of ABD-B homeodomain and analysis of *castor* promoter region

To examine whether BX-C directly interacts with the *caster* gene, we performed electrophoretic mobility shift assays (EMSA) using the *ABD-B* HD and oligonucleotides, which are located approximately within the 10 kb upstream of the *castor* gene. The *Abd-B* fragment containing HD was cloned into the pET30b expression vector (Fig. 2A), and the recombinant protein was purified. Coomassie staining of the purified protein indicated purity greater than 90% (Fig. 2B), and immunoblot analysis using anti-His·tag antibody confirmed the approximately 11 kDa protein of recombinant ABD-B HD, as indicated by an arrow in Fig. 2C.

Recently, it was reported that ABD-B HD binds to the responsive elements containing a canonical 5'-TTAT-3' core motif and a non-canonical 5'-TTAC-3' motif derived from the promoter region of the *yellow* gene (19). In addition, it has been identified that the upstream region of the *castor* gene contains seven conserved DNA sequence clusters to regulate the expression of *castor* gene in the embryonic brain and ventral nerve cord (20). Thus, we searched for the ABD-B binding motifs in the *castor* promoter region up to −10 kb, and found seven 5'-TTATGG-3' binding motifs and five 5'-TTACGA-3' binding motifs for ABD-B HD (Supplementary Table 2). Among them, we selected the most putative ABD-B binding sites for EMSA analysis: the cas1 containing 5'-TTAC-3' motif, the cas2 carrying 5'-TTAT-3' motif, and the cas3 containing two canonical core motifs which are overlapped by one thymidine (Supplementary Table 1). The 8-base pair core sequences of cas1 and cas3 have been reported as ABD-B binding sites in the promoter region of the *yellow* gene (19), and the core sequence of cas2 was analyzed as an ABD-B HD binding site in *cut*, *spalt*, and *unpaired* genes (11).

EMSA analysis and kinetic study

Generally, BX-C genes are mutually exclusive, so posteriorly expressed BX-C genes down-regulate the more anteriorly expressed ones on the embryonic surface. However, in the development of male and female sex organs and appendages, BX-C genes cooperatively interact with one another (21, 22).

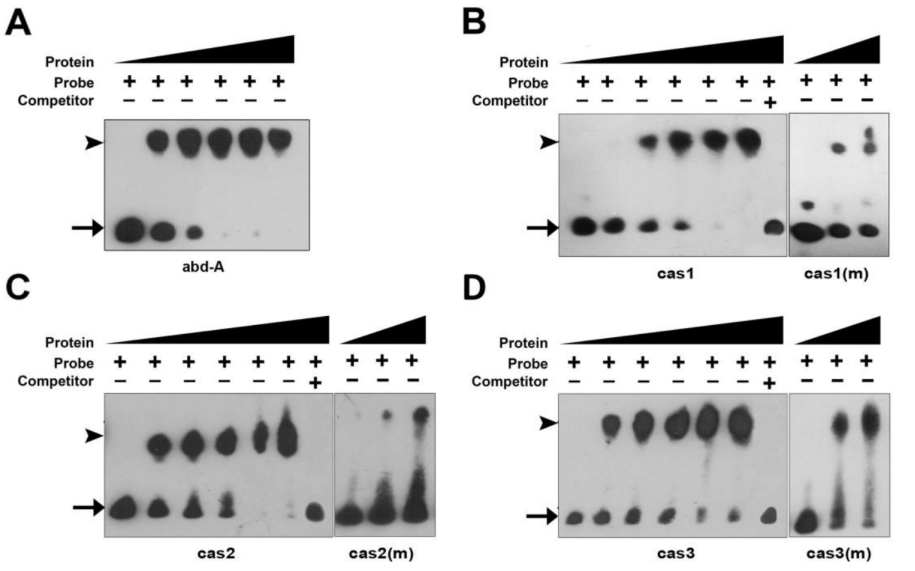

Fig. 3. EMSA analysis showing direct interaction of ABD-B homeodomain with the upstream promoter sequence of *caster gene*. The varying concentrations of the purified protein (0 nM, 0.62 nM, 1.25 nM, 2.5 nM, 5 nM, 10 nM from the left lane) were incubated with 10 fmol of abd-A probe (A), cas1 probe (B), cas2 probe (C), or cas3 probe (D). The protein-probe complexes were analyzed by electrophoresis on a native polyacrylamide gel. The protein-probe complexes are indicated by arrow heads, and the free probes are indicated by arrows. The competition assay was performed by using a 200-fold excess of cold probe that is not biotinylated, showing completely abolished band shifts (7^{th} lane in B, C, and D). The concentrations of the recombinant protein used for mutated probes (m) were 0 nM, 5 nM, and 10 nM from the left lane.

To examine the relationship between BX-C genes, the ABD-B binding site within the *abd-A* promoter region was analyzed by employing EMSA (Fig. 3A). The amount of protein-probe complexes is elevated as the concentration of ABD-B HD increases, demonstrating physical interaction between the recombinant ABD-B HD and abd-A probe.

Next, we explored whether ABD-B directly binds to the *castor* promoter region. The result showed that ABD-B HD interacted with all cas probes examined (Fig. 3B-D). In the competition assay adding a non-biotinylated cold probe with 200-fold excess molar concentration, no protein-probe complex was detected, indicating that the proteins specifically recognize the probe sequences. The specific interaction of ABD-B HD and cas probes was further confirmed using the cas(m) probes containing mutations within core binding motifs. The formation of the protein-probe complexes was significantly diminished in the cas(m) probes shown in the left panels in Fig. 3B-D, representing a sequence-specific interaction of ABD-B HD with the *castor* gene.

The binding affinities of the recombinant protein with its target sequences were measured by a luminescent image analyzer, and the equilibrium dissociation constant (K_d) was determined (Supplementary Fig. 1). The highest affinity of ABD-B HD was observed for the cas3 probe containing two 5'-TTAT-3' canonical core motifs (Table 1). This is consistent with a study in which a probe carrying more than one motif displayed higher affinity for ABD-B protein than that carrying only one motif (19). In addition, we revealed that the binding affinities for 5'-TTAT-3' and 5'-TTAC-3' core motifs did not differ much since cas1 and cas2 showed similar binding affinities. It should be noted that the binding affinity of cas1 for ABD-B HD is higher than that of the abd-A probe, although both probes contain the same 8-base pair core motif, implying that the flanking nucleotides are also involved in the interaction with ABD-B HD. It has been reported that the flanking bases contribute to the overall affinity and sequence specificity, possibly by interacting with the N-terminal flexible arm of the HD (6, 23). Therefore, we speculate that the flanking nucleotides of the abd-A probe are not favorable to the access of ABD-B HD. Taken together, we suggest that ABD-B can regulate the expression of *castor* transcripts by interacting with the *castor* promoter region.

In summary, we showed that BX-C genes are involved in regulating the expression of the *caster* gene by real-time PCR. Consistent with a previous study (18), ABD-B positively regulates *castor* gene expression, whereas UBX and ABD-A regulate *castor* gene expression negatively during embryonic stages 12 through 15. From the analysis of the *castor* promoter region, we selected the most putative ABD-B binding sites containing 5'-TTTTATGG-3' and 5'-TTTTACGA-3' core motifs for ABD-B HD. EMSA results showed that ABD-B HD specifically recognizes these sequences and directly binds to them. This is the first demonstration of the binding of ABD-B to the *castor* gene. The precise role of ABD-B in the regulation of *castor* expression needs to be addressed in future experiments.

MATERIALS AND METHODS

Drosophila strains and cross

Ubx$^{9.22}$, *abd-A*^{MX}, and *Abd-B*^{M2} carrying a loss-of-function mutation of BX-C genes, *scabrous-GAL4* (*sca-GAL4*) expressing GAL4 transcription factor in some proneural clusters and sensory organ precursor cells, and *Dr/TTG* (stock number 6663) were obtained from the Bloomington *Drosophila* Stock Center (Indiana). *UAS-UBX*, *UAS-abdA*, and *UAS-AbdB* were kindly provided by S. H. Jeon. To generate the homozygous null mutant embryos for bithorax genes, the *TM1* balancer chromosomes in the *Ubx*$^{9.22}$, *abd-A*^{MX}, and *Abd-B*^{M2} lines were replaced by *TTG* balancer chromosomes carrying P-element containing *twi-GAL4* and *UAS-2xEGFP*. The flies carrying one copy of bithorax mutant gene and *TTG* were crossed with each other, and the null embryos lacking a fluorescence signal were collected under a dissecting fluorescent microscope. To overexpress bithorax complex genes, *sca-GAL4* was crossed with each *UAS-Ubx*, *UAS-abdA*, or *UAS-AbdB* line. The Oregon-R strain was used as a wild-type control.

Real-time PCR

Embryos at each stage (12 through 15) were collected on an agar-grape juice plate with yeast paste. After dechorionation using 50% bleach solution, embryos were homogenized, and total RNA was extracted using an RNeasy Mini Kit (Qiagen). The purity and the amount of RNA were determined by nano micro-volume spectrophotometer (Maestro). cDNA was gen-

Table 1. Summary of relative affinity of the recombinant ABD-B homeodomain for various target sequences

Probe	Binding motif	Nucleotide position[a]	K_d (M)[b]	Fold compared to abd-A[c]
abd-A	5'-TTTTACGA-3'	−4,489	5.48×10^{-9}	1X
cas1	5'-TTTTACGA-3'	−7,410	2.98×10^{-9}	↑ 1.84X
cas2	5'-TTTTATGG-3'	−7,461	3.23×10^{-9}	↑ 1.70X
cas3	5'-TTATTATG-3'	−10,169	2.30×10^{-9}	↑ 2.38X

[a]Position of the 5' end of core motif is represented by the nucleotide number from the transcription start site according to flybase annotation. The binding motif of cas1 and cas3 is shown in reverse orientation. [b]The affinity was shown by K_d value, equilibrium dissociation constant. [c]The affinities for each cas probe are compared to that for abd-A probe.

erated from the total RNA by reverse transcription using oligo $(dT)_{18}$ primer and reverse transcriptase (Promega). To detect the expression levels of the genes *Ubx*, *abd-A*, *abd-B*, and *castor*, the cDNA was subjected to real-time PCR using an ABI 75100 sequencer detector (Applied Biosystems). The real-time PCR was performed using a StepOnePlus™ Real-time PCR System with Power SYBR Green PCR Master Mix (Applied Biosystems). The thermal cycling conditions were 95°C for 10 min, followed by 40 cycles of 95°C for 15 sec and 60°C for 60 sec. *Actin5C* was used as an internal control. The forward and reverse primers are shown in supplementary Table 1. The expression levels of *Ubx*, *abdA*, *AbdB*, and *castor*, either from the mutant or overexpressing embryos, were compared to those from wild-type embryos.

Plasmid construction and purification of ABD-B homeodomain

To express ABD-B HD, the *Abd-B* DNA fragment corresponding to amino acids 144 through 235 was amplified by polymerase chain reaction (PCR) using an *Abd-B* cDNA clone as a template, and BH-F and BH-R primers containing *Nde*I recognition sequence at the 5' end. The BH-F primer is 5'-GGCATATG*CAC CATCATCATCATCAT*TCCGTCCGGAAAAAGCGC-3' (the *Nde*I site is underlined, and italic letters represent histidine tag), and the BH-R primer is 5'-GGGCATATG*TCA*ATTGTTGTTGTTGG TTCTGCTGATTGGC-3' (the *Nde*I site is underlined, and italic letters represent stop codon). The PCR product was cloned into the *Sma*I site of the pBlueScript SK vector to produce a pB-BH recombinant construct. After the digestion of pB-BH with the *Nde*I restriction enzyme, the resulting fragment was cloned into an *Nde*I-digested pET30b bacterial expression vector to produce pET-BH.

The expression of the recombinant ABD-B HD in *E. coli* was carried out using a pET expression system (Novagen) according to the manufacturer's protocol with a minor modification. Briefly, the pET-BH plasmid was transformed into BL21(DE3), and the expression of the recombinant protein was induced by adding IPTG (isopropyl-β-D-thiogalactopyranoside) to a final concentration of 1 mM. After incubation for 3 h, the cells were collected and sonicated, and the recombinant protein was purified by affinity chromatography using a nickel-chelating column (24). The concentration and purity of the protein were determined by spectrophotometer and SDS-PAGE, respectively. The column-purified ABD-B HD was further dialyzed in phosphate buffered saline solution (PBS, 10 mM Na_2HPO_4, 1.8 mM KH_2PO_4, 2.7 mM KCl, 137 mM NaCl, pH 7.4), and used for EMSA experiments.

Immunoblot analysis

The samples from each column fraction were mixed with equal volumes of SDS sample buffer and boiled for 10 min. Ten micrograms of proteins were electrophoresed on an 8-14% gradient denaturing polyacrylamide gel, and transferred to PVDF membrane (Invitrogen) by electroblotting. The membrane was soaked in PBS buffer containing 0.2% casein and 0.1% Tween-20 for 1 h, and incubated with anti-His·tag antibody (1 : 250 dilution) (Applied Biological Materials Inc.) for 30 min. After incubation with the secondary antibody conjugated with biotin (1 : 500 dilution) for 30 min, the membrane was treated with streptoavidin conjugated with alkaline phosphatase (1 : 1,000 dilution) (Vector Laboratories) for 30 min. After washing the membrane with PBS containing 0.05% Tween-20, the membrane-bound ABD-B HD was visualized by adding NBT (Nitroblue tetrazolium chloride)/BCIP (5-bromo-4-chloro-3-indolyl phosphate) in neutralization buffer (0.1 M Tris-HCl, 0.1 M NaCl, pH 9.5).

EMSA

The biotinylated oligonucleotides containing ABD-B HD binding sequence were prepared (IDT) by analyzing the region 10 kb upstream of the *castor* gene. The forward and reverse oligonucleotides for each probe are shown in supplementary Table 1. For the preparation of the EMSA probe, biotinylated forward oligonucleotide was mixed with reverse oligonucleotide at equal molar concentrations. The mixture of oligonucleotides was annealed by heating at 95°C for 10 min, and slowly cooled down to room temperature to generate a double-stranded probe. In each reaction, 10 fmol probes were mixed with the purified ABD-B HD up to 10 nM in binding buffer containing 2.5% glycerol, 5 mM $MgCl_2$, 50 ng/μl poly (dI·dC), and 0.05% NP-40. After incubation of the reaction mixture at 25°C for 20 min, the samples were run on a non-denaturing 7% polyacrylamide gel in 0.5X TBE (45 mM Tris-HCl, 45 mM boric acid, 1 mM EDTA, pH 8.3), and transferred to a nylon membrane (Whatman).

EMSA reactions were carried out with a LightShift Chemiluminiscent® EMSA Kit according to the instructions (Pierce). In short, after cross-linking the probe to the membrane at 120 mJ/cm^2 using a crosslinker (Spectronics Corp.), the membrane was incubated in streptoavidin conjugated with horseradish peroxidase for 15 min. After washing the membrane, the protein-probe complex and free probe were detected by a Chemiluminescent Nucleic Acid Detection Module (Pierce), and visualized by X-ray film. The competition assay was performed by adding competitor DNA with 2 pmol of unlabeled oligonucleotide (200-fold excess) to the reaction mixture.

To determine the binding affinity of ABD-B HD with the probes, the band intensities were measured using an LAS-3000 luminescent image analyzer (Fuji Film), and the equilibrium dissociation constants (K_d) were determined using GraphPad Prism 4 software.

ACKNOWLEDGEMENTS

We would like to thank S. H. Jo for analysis of the data, and S. J. Kim for preparation of the manuscript. Special thanks to S. H. Jeon for providing *Drosophila* stocks. This research was supported by the Yeungnam University Research Grant (209A356024).

REFERENCES

1. Sharkey, M., Graba, Y. and Scott, M. P. (1997) *Hox* genes in evolution: protein surfaces and paralog groups. *Trands in Genet.* **13**, 145-151.
2. McGinnis, W. and Krumlauf, R. (1992) Homeobox genes and axial patterning. *Cell* **24**, 283-302.
3. Mann, R. S. and Morata, G. (2000) The developmental and molecular biology of genes that subdivide the body of *Drosophila*. *Annu. Rev. Cell Dev. Biol.* **16**, 243-271.
4. Sánchez-Herrero, E., Vernós, I., Marco, R. and Morata, G. (1985) Genetic organization of *Drosophila* bithorax complex. *Nature* **313**, 108-113.
5. Tiong, S., Bone, L. M. and Whittle, J. R. S. (1985) Recessive lethal mutations within the bithrax complex in *Drosophila*. *Mol. Gen. Genet.* **200**, 335-342.
6. Laughon, A. (1991) DNA binding specificity of HDs. *Biochemistry* **30**, 11357-11367.
7. Affolter, M., Percival-Smith, A., Müller, M., Leupin, W. and Gehring, W. J. (1990) DNA binding properties of the purified Antennapedia homeodomain. *Proc. Natl. Acad. Sci. U.S.A.* **87**, 4093-4097.
8. Ekker, S. C., Young, K. E., von Kessler, D. P. and Beachy P. A. (1991) Optimal DNA sequence recognition by the Ultrabithorax homeodomain of *Drosophila*. *EMBO J.* **10**, 1179-1186.
9. Yoo, S. (2010) Kinetic analysis of *Drosophila* Vnd protein containing homeodomain with its target sequence. *BMB Rep.* **43**, 407-412.
10. Ekker, S. C., Jackson, D. G., von Kessler, D. P., Sun, B. I., Young, K. E. and Beachy, P. A. (1994) The degree of variation in DNA sequence recognition among four *Drosophila* homeotic proteins. *EMBO J.* **13**, 3551-3560.
11. Lovegrove, B., Simoes, S., Rivas, M. L., Sotillos, S., Johnson, K., Knust, E., Jacinto, A. and Hombria, J. C.-G. (2006) Coordinated control of cell adhesion, polarity, and cytoskeleton underlies Hox-induced organogenesis in *Drosophila*. *Curr. Biol.* **16**, 2206-2216.
12. Celniker, S. E., Keelan, D. J. and Lewis, E. B. (1989) The molecular genetics of the bithorax complex of *Drosophila*: characterization of the products of the *Abdominal-B* domain. *Genes Dev.* **3**, 1424-1436.
13. Delorenzi, M. and Bienz, M. (1990) Expression of *Abdominal-B* homeoproteins in *Drosophila* embryos. *Development* **108**, 323-329.
14. Boulet, A. M., Llyoyd, A. and Sakonju, S. (1991) Molecular definition of the morphogenetic and regulatory functions and the *cis*-regulatory elements of the *Drosophia Abd-B* homeotic gene. *Development* **111**, 393-405.
15. Mellerick, D. M., Kassis, J. A., Zhang, S. D. and Odenwald, W. F. (1992) Castor encodes a novel zinc finger protein required for the development of a subset of CNS neurons in *Drosophila*. *Neuron* **9**, 789-803.
16. Cui, X. and Doe, C. Q. (1992) *ming* is expressed in neuroblast sublineages and regulates gene expression in the *Drosophila* central nervous system. *Development* **116**, 943-952
17. Fontana, J. R. and Crews, S. T. (2012) Transcriptome analysis of *Drosophila* CNS midline cells reveals diverse peptidergic properties and a role for *castor* in neuronal differentiation. *Dev. Biol.* **372**, 131-142.
18. Ahn, J.-H., Yoo, S., Park, H.-J., Jung, K.-I., Kim, S.-H. and Jeon, S.-H. (2010) *Drosophila castor* is regulated negatively by the *Ubx* and *abdA* genes, but positively by the *AbdB* gene. *Int. J. Dev. Biol.* **54**, 1251-1258.
19. Jeong, S., Rokas, A. and Carroll, S. B. (2006) Regulation of body pigmentation by the Abdominal-B Hox protein and its gain and loss in *Drosophila* evolution. *Cell* **125**, 1387-1399.
20. Kuzin, A., Kundu, M., Ross, J., Koizumi, K., Brody, T. and Odenwald, W. F. (2012) The *cis*-regulatory dynamics of the *Drosophila* CNS determinant *castor* are controlled by multiple sub-pattern enhancers. *Gene Exp. Patterns* **12**, 261-272.
21. Casares, F., Calleja, M. and Sánchez-Herrero, E. (1996) Functional similarity in appendage specification by the *Ultrabithorax* and *abdominal-A Drosophila* Hox genes. *EMBO J.* **15**, 3934-3942.
22. Foronda, D., Estrada, B., de Navas, L. and Sánchez-Herrero, E. (2005) Requirement of *abdominal-A* and *Abdominal-B* in the developing genitalia of *Drosophila* breaks the posterior downregulation rule. *Development* **133**, 117-127.
23. Gruschus, J. M., Taso, D. H. H., Wang, L.-H., Nirenberg, M. and Ferretti, J. A. (1997) Interaction of the vnd/NK-2 homeodomain with DNA by nuclear magnetic resonance spectroscopy: Basis of binding specificity. *Biochemistry* **36**, 5372-5380.
24. Yoo, G.-W. and Shin, C.-G. (2013) Biochemical characteristics of functional domains using feline foamy virus integrase mutants. *BMB Rep.* **46**, 53-58.